Zeitschrift: IABSE reports of the working commissions = Rapports des commissions de travail AIPC = IVBH Berichte der Arbeitskommissionen

Band: 34 (1981)

Artikel: Fracture mechanics analysis of discrete cracking

Autor: Saouma, Victor E. / Ingraffea, Anthony R.

DOI: https://doi.org/10.5169/seals-26905

Fracture Mechanics Analysis of Discrete Cracking

Analyse par la mécanique de rupture de la propagation des fissures distinctes

Bruchmechanische Behandlung diskreter Rissausbreitung

VICTOR E. SAOUMA
Post-Doctoral Research Associate
Dept. of Civil Engineering
Princeton University
Princeton, NJ, USA

ANTHONY R. INGRAFFEA
Assistant Professor and Manager
of Structural Research
Dept. of Structural Engineering
Cornell University
Ithaca, NY, USA

SUMMARY
A completely new and comprehensive solution to the problem of discrete crack m@delling using fracture mechanics concepts is described. The solution predicts the trajectory and stability of any number of cracks propagating in mixed-mode. Remeshing and renumbering are done automatically. Analysis is performed in an interactive computer graphics environment. Example problems are presented.

RÉSUMÉ
Une solution exhaustive et nouvelle de la modélisation des fissures distinctes employant la mécanique de rupture est présentée. La solution prédit la trajectoire et la stabilité de plusieures fissures se propageant suivant une direction arbitraire. Le maillage du réseau est ajusté automatiquement.
L'analyse est accomplie au moyen d'un traitement interactif et graphique. Des exemples sont présentés.

ZUSAMMENFASSUNG
Eine ganz neue, wie auch umfassende Lösung des Problems des diskreten Bruchmodellierens mittels bruchmechanischer Begriffe wird beschrieben. Die Lösung beschreibt Richtung und Stabilität von Rissen, die bei gemischten Brucharten auftreten. Neueinteilung und Neunummerierung der Elementeneinteilung wird automatisch ausgeführt. Die Behandlung geschieht in einem dialogfähigen Graphikcomputer. Probleme werden exemplarisch behandelt.

1. INTRODUCTION

In two of the introductory reports presented at this colloquium, the increasing importance of applying fracture mechanics to the study of cracking in reinforced concrete is emphasized. Bazant [1] shows that objectivity in predicting fracture initiation is satisfied if fracture toughness, rather than the currently employed tensile strength, is used as a measure of resistance to crack growth. On the issue of discrete versus smeared crack modelling, Bazant [1] argues for the smeared approach. He states that a numerically smeared representation is more realistic, and, moreover, precludes the need to update mesh topology and connectivity with each increment of cracking.

Argyris, Faust, and Willam [2] concur with Bazant's [3] findings on the objectivity of fracture toughness as a cracking criterion. They, like Bazant [1], list the relative merits of discrete versus smeared crack representations but appear to favor the former approach [4].

Together, the two papers highlight the pressing need for research into the following areas of application of fracture mechanics to reinforced concrete:

1. Topology: If a discrete crack model is to be used, a method of regeneration of the finite element mesh to accommodate incrementally changing crack trajectories must be found. This method must introduce the appropriate displacement and traction discontinuities across the crack, must properly account for required meshing near the crack tips, and, ideally, should minimally disturb the bandedness of the system stiffness matrix in accounting for element connectivity changes. Moreover, the method must be fast and user-friendly.

2. Singularity: A linear elastic fracture mechanics approach to discrete cracking requires recognition of the theoretically singular nature of the crack tip stress field. If fracture toughness, K_{Ic}, is to be the controlling material parameter, stress intensity factors K_I, K_{II}, K_{III}, the coefficients of the singular stress terms, must be found for a given crack configuration and loading. In the finite element context, this implies the ability to compute accurately and efficiently the stress intensity factors through proper near-tip meshing.

3. Stability: Cracking in reinforced concrete is not always catastrophic because stable growth always occurs before global instability as a result of the crack arresting effect of the steel. Neither is it always in pure Mode I, since cracking is generally curvilinear due to mixed-mode action. For a given load increment on a structure with multiple cracks, methods must be available for predicting the length and direction of the corresponding crack increments.

In response to this call for research this paper presents, for the first time to the authors' best knowledge, a comprehensive solution to the problem of discrete crack modelling using fracture mechanics concepts. It will be shown that the solution is comprehensive in the sense that it satisfies all of the requirements listed above under topology, singularity, and stability for problems which can be modelled as two-dimensional or axisymmetric.

In solving the problems of topology, the present method employs automatic mesh regeneration and bandwidth minimization algorithms. The developed code operates in a medium-level, i.e. storage-tube, interactive computer graphics environment. The primary objective here is to completely eliminate the strongest drawback to discrete crack modelling: manual remeshing and renumbering. An equally important objective, however, is to take advantage of the rapidly developing techniques and hardware of computer graphics to put the engineer back into

structural analysis. Analyses which involve physically complex processes such as crack propagation are least effectively done in a "black-box" environment. The user should be allowed to observe the analysis and inject his judgment into it as appropriate while it is in progress. Examples of automatic remeshing and other aspects of the interactive nature of the present program are contained in this paper.

The present solution is predicated on the applicability of linear elastic fracture mechanics to concrete cracking. Consequently, a key aspect of the analysis process is automatic computation of mixed-mode stress intensity factors, K_I and K_{II}, at the tip of each crack. The method used has been shown to be highly accurate and efficient in other areas of fracture.

The questions of stability and crack increment direction are answered in the present approach by use of recent developments in mixed-mode crack initiation theory. The length of a crack increment is computed through a recently developed energy balance algorithm. When the length and direction of each crack increment is computed, the necessary topology changes are known and the automatic mesh generator and bandwidth minimizers are invoked for the next cycle of loading. Again, details of these methods, as well as results of example problems are presented in this paper.

It will be shown that a thoroughly new and comprehensive tool for analysis of certain classes of reinforced concrete structures has been created. In comparison with currently popular analysis programs, the present one is as efficient and accurate, but much more friendly and appealing to the analyst.

2. THEORETICAL BACKGROUND

2.1 Crack Stability

The question of applicability of a single-parameter, K_{Ic}, to the onset of Mode I crack propagation in concrete has had a checkered history. Reference to many publications addressing this question was made in a recent report by the authors [5] in which they concluded that a classical fracture mechanics approach can indeed be valid if, as in testing of metals, certain geometrical conditions are met. It is the authors' contention that for materials in which a microcracking process zone is created at the crack tip:

1. A valid K_{Ic} can be measured using standard techniques such as ASTM E 399-80 [5,6,7,8].

2. Of the geometrical conditions to be met in such testing, the most important is that crack length, a, be large compared to maximum, aggregate size, d_{max} [7,8].

3. The ratio a/d_{max} can be as small as four or five in tests which would yield a K_{Ic} valid for structural engineering purposes.

4. Contrary to Bazant's [1] blunt crack band approach, the observed [8,9] process zone size is a small percentage of crack length at crack tip instability. In tests on concrete [9], the process zone size has been observed to be only a few millimeters in length.

Consequently, a classical linear elastic fracture mechanics approach to crack instability in Mode I is taken in the present model. That is, when the computed stress intensity factor, K_I, reaches the value of the concrete fracture toughness, K_{Ic}, a necessary and sufficient condition for local instability is met.

It should be recalled, however, that cracks rarely propagate in concrete structures in pure Mode I. In the present model the local stability of a crack loaded in mixed-mode is approached through substitution of the computed K_I and K_{II} into a theoretical interaction formula. The formula used in the analysis of the problems presented in this paper was developed by Erdogan and Sih [10]. It states that fracture initiation is dependent on the circumferential tensile stress, $\sigma(\theta)$, (Fig. 1) near the crack tip and that fracture initiates from the crack tip in a direction normal to $\sigma(\theta)_{max}$. The $\sigma(\theta)_{max}$ theory predicts an interaction in the K_{Ic}-normalized K_I-K_{II} plane according to,

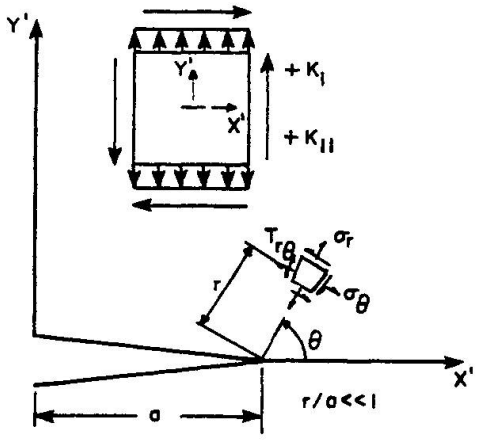

Fig. 1 Crack-Tip Stress Notation

$$\cos\frac{\theta_o}{2}\left[\frac{K_I}{K_{Ic}}\cos^2\frac{\theta_o}{2} - \frac{3}{2}\frac{K_{II}}{K_{Ic}}\sin\theta_o\right] = 1 \qquad (1)$$

The fracture angle, θ , is found by maximizing the expression for the circumferential stress around a crack tip, yielding:

$$\cos\frac{\theta_o}{2}\left[K_I\sin\theta_o + K_{II}(3\cos\theta_o - 1)\right] = 0 \qquad (2)$$

Many mixed-mode fracture initiation theories have been proposed recently and three of the most widely accepted theories have been made available in the code: 1) the maximum circumferential stress theory, 2) the maximum energy release rate theory ($G(\theta_{max})$) [11], which states that the crack will grow in the direction along which the elastic energy release rate will be maximum, and the crack will start to grow when this energy release rate reaches a critical value, and 3) the minimum strain energy density theory ($S(\theta_{min})$) [12] which states that the crack will extend in the direction along which the strain energy density at a critical distance is a minimum when this minimum reaches a critical value.

2.2 Crack Increment Length

Thus far, only the problem of local stability has been considered. That is, the substitution of K_I, K_{II} and K_{Ic} into any of the three mentioned theories will indicate whether a crack will extend, and its angle of propagation.

It is important to realize that a crack extension, or local instability, is not synonymous with failure or with global instability. This is because a crack may be unstable only for a certain crack extension length. Due to the stress redistribution accompanying the crack propagation (a form of geometric non-linearity), its stress intensity factors may decrease resulting in an eventual crack arrest. Alternatively, as a crack crosses reinforcement, the steel acts as a crack arrestor and decreases the stress intensity factors.

An algorithm for computing the length of each increment of cracking caused by an increase in load was first proposed by Ingraffea [15]. In the present case, the problem was addressed from a different point of view; the load increase which forces a crack to extend a given distance in a quasi-stable way was computed. The scheme is based on the release of potential energy to form surface energy. The energy required to create a new unit of surface area is a material constant

related to its fracture toughness by:

$$R = \frac{K_{Ic}^2}{E'}$$

$$\text{where } E' = E \qquad \text{for plane stress} \qquad (3)$$

$$E' = \frac{E}{(1-\nu^2)} \qquad \text{for plane strain}$$

The direct determination of the energy released, $G(\theta)$, during the propagation of a crack at an arbitrary angle had been a mathematical challenge for many years. Of the many solutions now becoming available, that of Hussain et al. [11] is employed in the present analysis.

If for a given crack configuration G is greater than R, a local instability occurs and the crack will extend. As the crack propagates, G may increase, resulting in an unstable crack growth or global instability. Alternatively, G may decrease and lead to stable crack growth.

For stable crack growth, the question is then how far the crack extends under a given fixed load before it stops. It is clear that an equilibrium state will be reached when a balanced energy transfer occurs from G to R, as shown in Fig. 2, in the following form.

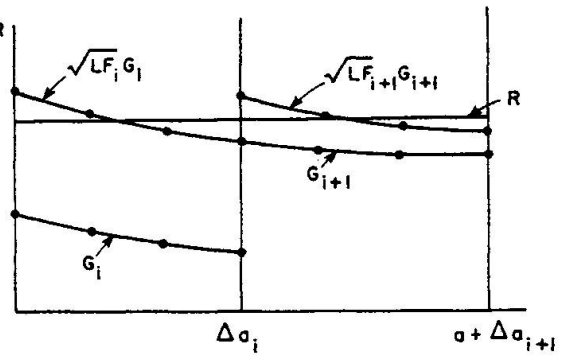

Fig. 2 Graphical Form of Energy Balance Algorithm for Crack Length Prediction

$$\int_o^{\Delta a^*} G(a,\theta,K_I,K_{II})\, d\Delta a = \int_o^{\Delta a^*} R(K_{Ic})\, d\Delta a \qquad (4)$$

where Δa^* represents the point of crack arrest.

In the present investigation, the problem consists in determining the load amplification factor which will cause the initial crack to extend by a predefined increment, Δa^*.

Given a structure, analyzed for four crack positions all with the same load P_i, a curve through the four corresponding values of G can be defined. The area under the G-curve, A_G, is the amount of energy released, and the area under the R-curve, A_R, is the amount of energy needed to create a new surface area corresponding to the crack increment Δ^*.

If A_G is greater than A_R, then a form of instability occurs. It will be a local instability if G decreases with crack length and the energy balance transfer will be satisfied before the crack reaches a free surface. Alternatively, if G increases with crack extension, then a global instability and failure take place.

If A_G is smaller than A_R, then to satisfy the energy balance transfer, A_G should be increased by appropriately shifting the G-curve upward. Since G is proportional to the square of stress intensity which in turn is directly proportional

to the load, the load amplification factor for the current increment will be:

$$LF = \sqrt{\frac{A_R}{A_G}} \tag{5}$$

The determination of A_G is accomplished by dividing each crack increment into three sub-increments, each with its own direction and value of G, fitting a curve through the four G-values, and integrating the resulting expression over the crack increment length. This is done automatically for each crack increment.

2.3 Stress Intensity Factor Calculations

To ascertain the stability, direction, and length of a crack increment, the stress intensity factors must be known. The problem here is twofold: (a) modelling the appropriate form of singularity by special elements, and (b) the extraction of the stress intensity factors from the near-tip displacement field.

The development of a reliable, simple and "cost effective" singular element had to wait until 1975 when, concurrently, Barsoum [13] and Henshall and Shaw [14] discovered the fortuitously singular nature of the quarter-point, quadratic, isoparametric quadrilateral and triangle.

Since the quadratic displacement interpolation functions are not in any way altered in creating the $r^{-1/2}$ stress singularity in the element, use of this offset-node geometry does not change the element convergence characteristics. Moreover, the element stiffness matrix is formulated by the same subroutine as usual; only the nodal coordinate input data are altered.

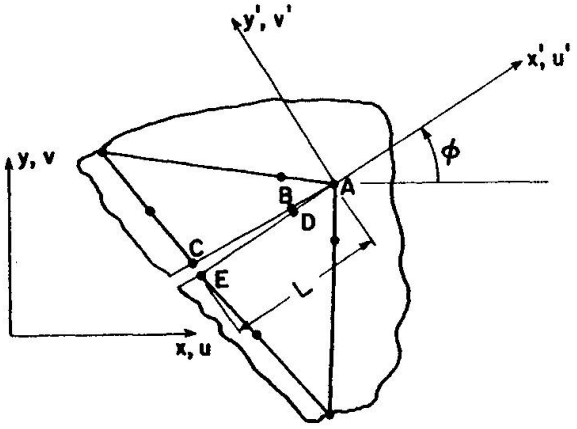

Fig. 3 Crack-Tip Element Nodal Lettering Scheme

The displacement correlation method [15,16] is employed for determination of stress-intensity factors from the nodal displacements of the singular elements. Denoting the local displacements along the crack axis as U' (crack sliding displacement, CSD) and the displacement normal to the crack axis as V' (crack opening displacement, COD) the stress intensity factors can be directly evaluated from:

$$K_I = \frac{G}{\kappa+1}\sqrt{\frac{2\pi}{L}}\left[4(V'_B - V'_D) + (V'_E - V'_C)\right]$$

$$K_{II} = \frac{G}{\kappa+1}\sqrt{\frac{2\pi}{L}}\left[4(U'_B - U'_D) + (U'_E - U'_C)\right] \tag{6}$$

where $\kappa = \frac{(3-\nu)}{1+\nu}$ plane stress

$\kappa = 3 - 4\nu$ plane strain

with reference to Fig. 3. Examples of the accuracy and simplicity of this method can be found in References 17 and 18.

3. PROGRAM DESCRIPTION

With the objective of modelling discrete crack propagation in reinforced concrete, the theoretical developments outlined above were incorporated into a program entitled FEFAP (Finite Element Fracture Analysis Program). Its general capabilities are described in this section.

3.1 Element Library

Concrete is modelled by quadrilateral or triangular quadratic isoparametric elements. Main steel reinforcement is modelled by quadrilateral elements which provide both axial and bending stiffness. Three-noded linear elements are used for shear reinforcement. Bond between the concrete and steel and aggregate interlock along cracks are modelled by an isoparametric version of the interface element developed by Goodman et al. [19,20].

3.2 Constitutive Models

While the initial objective of this investigation was restricted to a linear elastic concrete model, it was found from test problems that the response under high loads was too stiff. This was attributed to the constant value assigned to the concrete Young's modulus.

The code was extended to account for material softening as dictated by an appropriate model. A simple model which would encompass both the biaxial and triaxial state of stress (for plane strain and axisymmetric analyses) for the failure criterion and the prediction of the secant Young's modulus and Poisson's ratio was selected and implemented. The secant values are needed because load is always applied in a single increment, as will be indicated below. The selected failure criterion, proposed by Ottosen [21,22], is based on a four-parameter equation containing explicitly all the three stress invariants.

The steel model is currently linear elastic.

Steel-concrete bond was governed by the equation developed by Nilson [23].

Finally, the aggregate interlock model requires special comment. It has been recognized that the shear modulus along a crack is a portion, α, of the inital uncracked modulus. Theoretically, α should be inversely proportional to the crack opening, but such a relative displacement is not directly derived in the general smeared cracked model. The present model takes advantage of the discrete nature of the crack to directly compute the crack opening and accurately evaluate the shear stiffness along the crack using the empirical equation derived by Fenwick and Paulay [24].

3.3 Program Capabilities

To model discrete crack propagation, in plane and axisymmetric structures, the following capabilities were implemented:

1. An automatic element and node generation capability for regular meshes.

2. An automatic nodal adjustment for the singular elements, and direct extraction of the stress intensity factors.

3. A graphical display capability on a TEKTRONIX 4013 or 4014 terminal.

4. Forms of loading: a) nodal, b) edge, c) initial nodal displacement, d) gravity, and e) thermal.

5. A mesh optimizer for bandwidth minimization and direct nodal renumbering [25,26].

6. A highly efficient In/Out of core skyline-banded equation solver [27].

7. Graphical display of the deformed mesh, the principal stresses, and the cracking pattern.

8. A completely interactive means of operation within the program.

9. Automatic, discrete crack nucleation at arbitrary points, on an edge or in the interior of a domain, and angles as specified by the analysis.

10. Automatic, discrete crack propagation capability with mesh adjustment along the propagating crack.

11. User interaction with the code to perform interactively final minor adjustments to each regenerated mesh.

These capabilities required about 9000 FORTRAN statements grouped in 80 subroutines.

A detailed scenario of the analysis procedure is too long to include in this paper. It can be found in Reference 28. Some further details of the mesh regeneration accompanying crack propagation are, however, included in the next section.

4. DISCRETE CRACK PROPAGATION MODELLING

The essential requirement of the present model is the availability of a set of routines which will control the mesh modification caused by an arbitrary extension of an interelement crack.

4.1 General Strategy

The general strategy followed for the crack extension through a finite element mesh is as follows:

1. From the initial direction of the crack axis, and the predicted angle of crack extension with respect to the crack direction, determine the angle of crack propagation in global coordinates.

2. Replace the quarter-point nodes to their initial midside position, to remove the local singularity.

3. Define a new crack tip node whose coordinates are determined from the length and angle of crack extension.

4. Define a new node adjacent to the old crack tip node.

5 Search the previous singular elements, to determine which one is going to be crossed by the crack.

6. If the new crack tip node falls inside this element, extend the crack to it and go to 8, otherwise simply extend the crack through the entire length.

7. Locate the next element to be crossed by the crack and go to 6.

8. Define the new nodes from which the stress intensity factors will be evaluated.

9. Adjust the midside nodes to the quarter-point position, where needed.

10. Display the modified mesh, to allow the user to interactively perform final adjustments.

11. Evaluate the stiffness matrices of those elements perturbed or newly created by the mesh modification.

4.2 Actual Implementation

The actual implementation of the above mentioned strategy rests on three main requirements:

1. To handle a discrete crack crossing an element.

2. Once a crack emerges from an element, to find out which element is the next to be entered.

3. Check if the crack will stop in the next element to be entered.

In the most general case, the crack may cross a triangular or a quadrilateral element in different ways. The crack may enter from a node or a side, leave from another node or another side or simply stop inside it. Thus a number of different situations may arise where some adjustments are required, and all possible combinations have to be accounted for.

The 25 possible cases are schematically shown in Fig. 4.

Once a crack has emerged from an element side or node, a search is performed to locate which of the elements is going to be entered next, and (if so) whether the crack is going to stop in it.

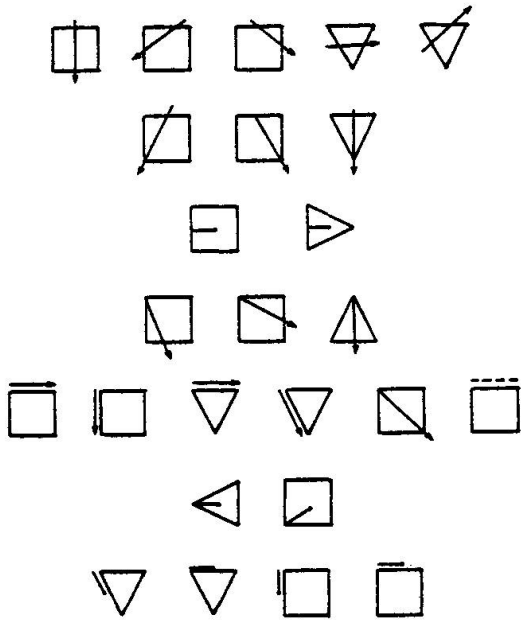

Fig. 4 Possible Crack Paths Across, Into, and Around Elements

4.3 Corrective Measures

A number of pathological situations may arise, and if properly diagnosed, special corrective measures will automatically be taken by the code. Those corrections occur:

1. When a crack is about to cross a bond or steel element. Since steel elements can obviously not be broken by the crack, special modifications which will ensure subsequent displacement continuity will be performed (see Fig. 5).

2. When a crack extends through an element by breaking it in two (the most general case), and one of the resulting elements has a very large aspect ratio, then one of the sides of the original element will be shifted. This will allow the crack to propagate between two adjacent elements and will further require the adjustment of some of the midside nodal coordinates and the reevaluation of the stiffness matrices of the elements sharing the shifted side.

3. When a crack tip stops close to a side or to a node, then elements with a poor aspect ratio will be generated and some modification will be necessary.

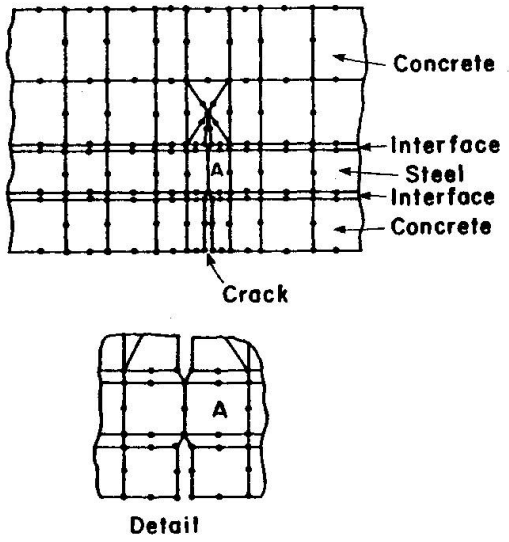

Fig. 5 Topology Around Crack Which Crosses Main Reinforcement. Interface Elements Model Bond.

Even though much effort has been made to automate the progressive crack growth and nucleation procedure, no claim can be made that the method will cover every possible cracking condition encountered in every analysis. In fact engineering judgment should remain an essential and ultimate part of the analysis. To this end, the user, based on a picture display of the modified mesh, can interactively take appropriate corrective measures. These include the dragging of a node from one position to another, or changing a diagonal common to two triangular elements, to improve their aspect ratios.

4.4 Discrete Crack Nucleation

If a crack is to nucleate at a certain Gauss point of a particular element, the following steps will be performed:

1. The direction of the new crack is displayed on the screen for approval by the user who may reverse its direction by 180 degrees.

2. The user is prompted to locate the node where the crack is to nucleate.

3. The program will generate a new node adjacent to the indicated one.

4. From that point on, the code will treat the problem as if it were asked to propagate a crack emanating from a node. This process will be applied once (if the crack nucleates from a free surface), or twice (if the crack nucleates from the interior). The initial crack size is arbitrary; the crack tip is located in such a way that its distance from the nucleating node is equal to half the closest element side length.

5. Singular element angles are checked and adjusted if necessary.

6. Once the crack has been nucleated, the user can either reduce its length by shifting the crack tip node, or extend it by asking for a complete crack extension run.

5. EXAMPLE PROBLEMS

As an integral part of their research program on the shear strength of reinforced concrete beams, Bresler and Scordelis performed a number of experimental tests. Those tests were so accurately performed and so thoroughly recorded [29,30] that their primary objective has been overshadowed by their use as a yardstick to evaluate many, if not most, finite element reinforced concrete codes. Beam OA-1 of their test series is here analyzed as an example of the capabilities of FEFAP.

5.1 Problem Description

The experimental setup of the beam and its dimensions are shown in Fig. 6. The beam was reported to have:

Thickness: 12 in. (305 mm)
Concrete compressive strength: 3.27 ksi (22.6 MN/m^2)
Concrete secant modulus: 3,470 ksi (23.9 GN/m^2)
Concrete modulus of rupture: .575 ksi (3.96 MN/m^2)
Concrete Poisson's ratio: .15
Steel yield stress: 82 ksi (566 MN/m^2)
Longitudinal reinforcement: 4 #9 bars
Vertical reinforcement: None

The steel bars were bolted to a plate at each end of the beam to prevent bond failure due to possible insufficient anchorage after the formation of diagonal tension cracks.

The beam was reported to have failed in a diagonal tension failure mode at a load of 58 kips (258 KN). The final observed crack pattern, Fig. 7, indicates that five major cracks had developed on each side of the center line. It should be noted that the beam had a steel ratio of 1.8 percent, well above the balanced one of 1.4 percent.

5.2 FEFAP Analysis

Four different analyses of this problem have been performed. The varying parameters were: 1) concrete material model, 2) fracture toughness, 3) shear transfer along the crack. Since the beam was overreinforced, and the steel bars were bolted at each extreme, bond was not expected to play a major role and was not considered as a variable in the present investigation. Descriptions of the four analyses are summarized in Table 1.

TABLE 1. Description of Analyses Performed

	Concrete Model	Shear Transfer Along Crack	Fracture Toughness ($lb\text{-}in^{-3/2}$)	Fracture Toughness ($MNm^{-3/2}$)
L-AI-600	Linear	Yes	600.	0.66
L-NAI-600	Linear	No	600.	0.66
L-AI-1200	Linear	Yes	1200.	1.32
NL-AI-600	Non-linear	Yes	600.	0.66

After a description of the finite element idealization, the results of each analysis will be presented, discussed, and compared with other results.

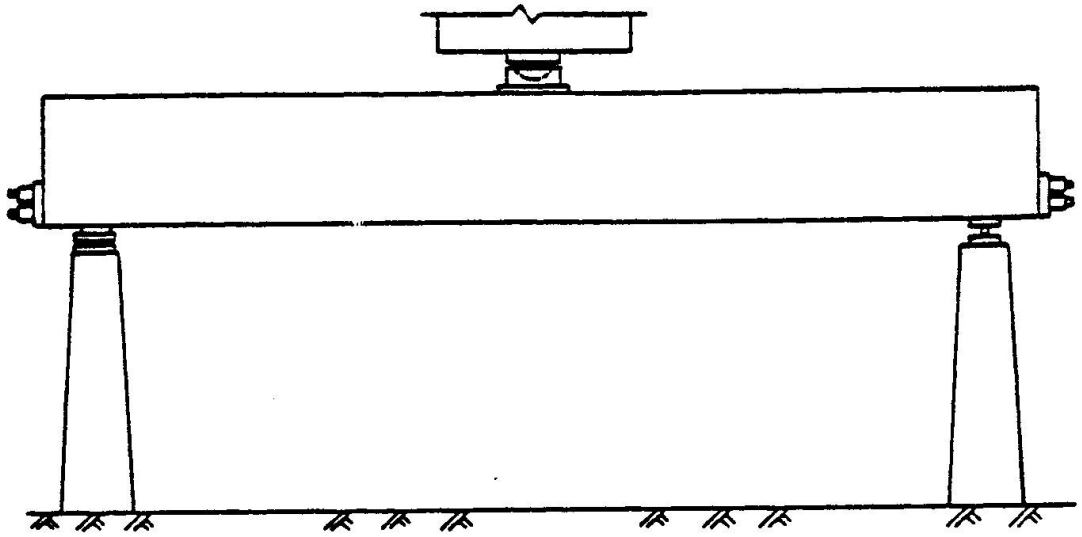

Fig. 6 Testing Configuration of Beam OA-1 [29,30]

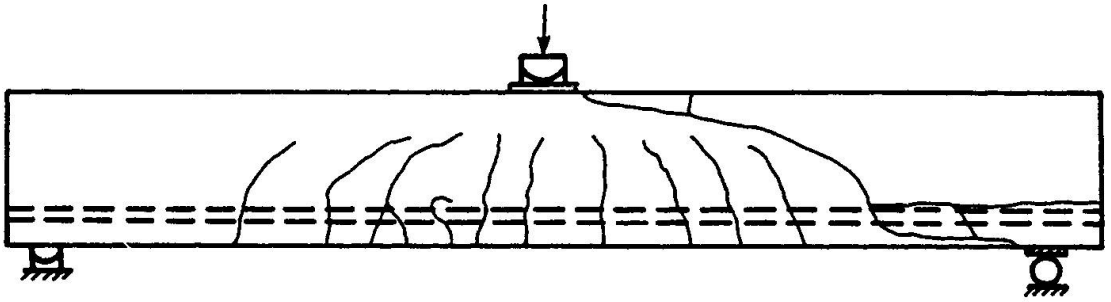

Fig. 7 Observed Crack Pattern on Beam OA-1 [29,30]

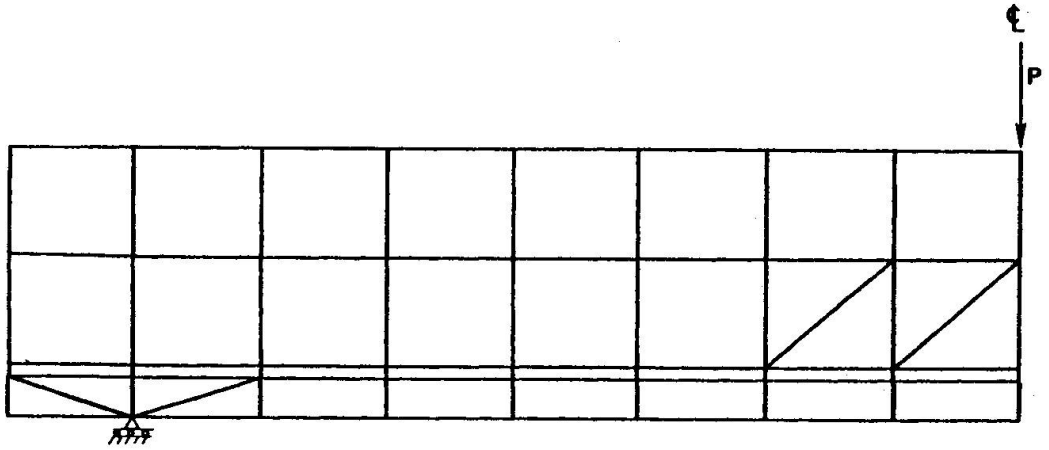

Fig. 8 Initial FEFAP Finite Element Idealization of Beam OA-1

5.2.1 Finite Element Idealization

The smooth stress gradients in an uncracked beam, the accuracy provided by the isoparametric quadratic elements, and the obvious objective of minimizing the initial number of nodes, allowed the selection of the initial mesh shown in Fig. 8. Interface elements are spread along both sides of the steel layer except for the last steel element next to the anchorage.

The only restriction imposed by the selection of an initial mesh is the minimum distance between two adjacent cracks [approximately 10 inches (254 mm)]. This is imposed by the present code limitation to nucleate a crack from an element corner node only. The local mesh refinement below the load point was initially implemented to allow the simultaneous occurrence of two adjacent cracks with the same initial length without their having a common singular element.

The $\sigma(\theta)_{max}$ theory [10] was used throughout the analyses as the mixed-mode fracture criterion.

5.2.2 Finite Element Results

Results of each analysis will be individually reported as follows:

1. A plot of the final deformed mesh.
2. A plot outlining the final crack pattern.
3. A figure of the final load-displacement curve.

These results are shown in Figures 9 through 12. With reference to those figures, the following general comments may be made:

1. The simple linear model with aggregate interlock, Fig. 9 is satisfactory up to a load of about 40 kips (178 KN) [where the maximum computed compressive stress reaches a value of 1900 psi (13.1 MN/m^2)]. The discrepancy above this load is attributed to the constant elastic modulus assigned to the concrete.

2. The second analysis, Fig. 10, differing from the first only in the value of K_{Ic}, shows a definitely stiffer response than the previous one.

This difference can easily be explained by recalling that the load forcing a crack to extend is directly proportional to fracture toughness. If two identical structures are subjected to similar loads, the one with the lower fracture toughness will be more extensively cracked and thus exhibit a softer response than the other. This is reflected by the larger load (84.5 kip vs 64.5 kip, 376 KN vs 287 KN) required to crack this beam less extensively than L-AI-600.

It is important, however, to note the relatively low sensitivity of the load-displacement curve to a large change in the value of the fracture toughness. One may conclude that a realistic value is really all that is needed. Of course, if prediction of a crack tip location as a function of the load is required, then great care should be exercised in selecting a proper value for the fracture toughness.

3. The third analysis, Fig. 11, produced, initially, a good load displacement correlation with the experimental results. However, it became apparent from the evolving crack configuration that unrealistic crack paths were being followed. The analysis was interrupted when it became clear that two cracks were about to intersect with each other; this could not have been modelled by the present version of FEFAP.

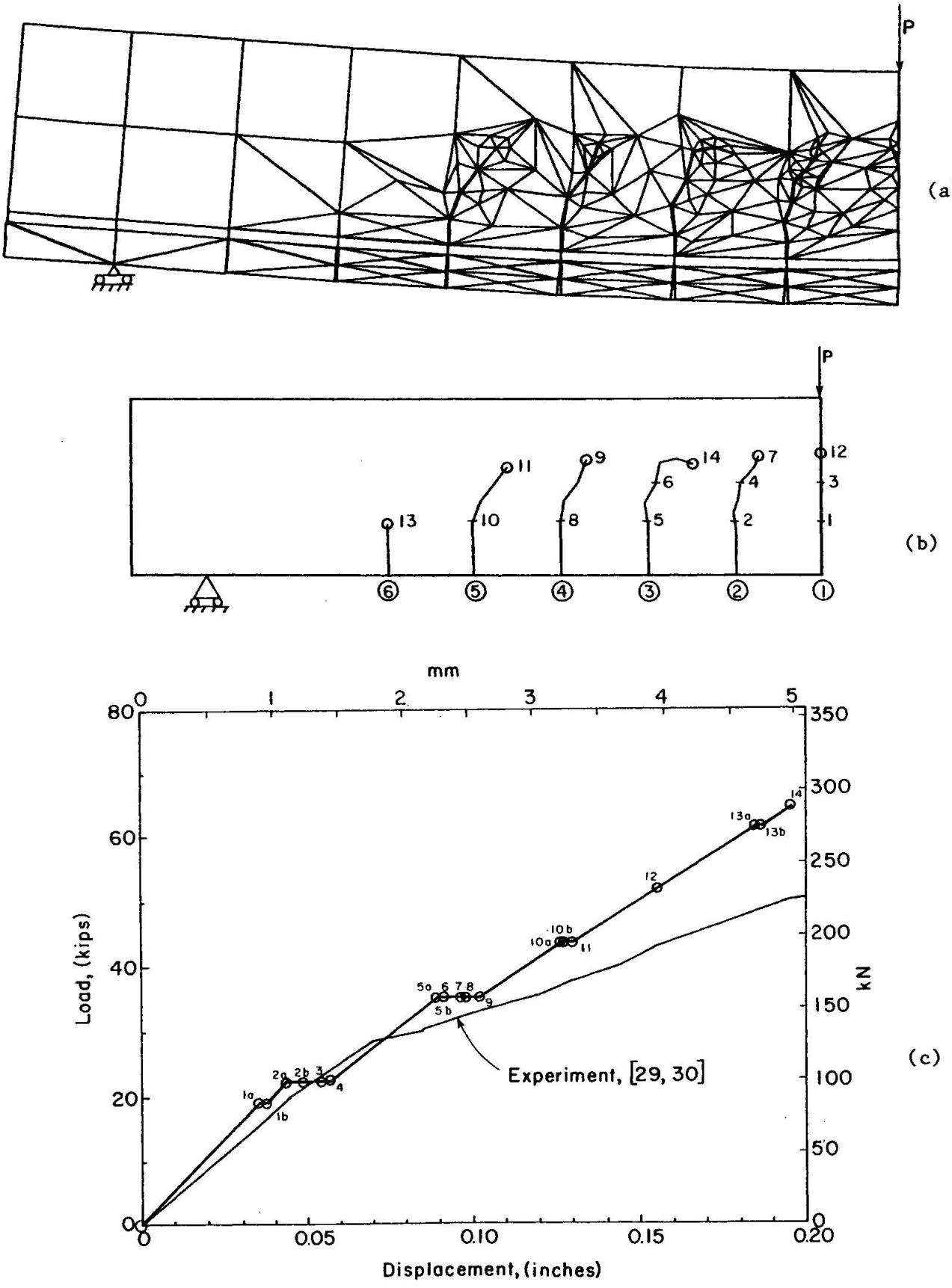

Fig. 9 Results of Analysis L-AI-600. a) Final Mesh on Deflected Shape b) Final Crack Pattern c) Comparison of Calculated and Observed Load-Displacement Curves.

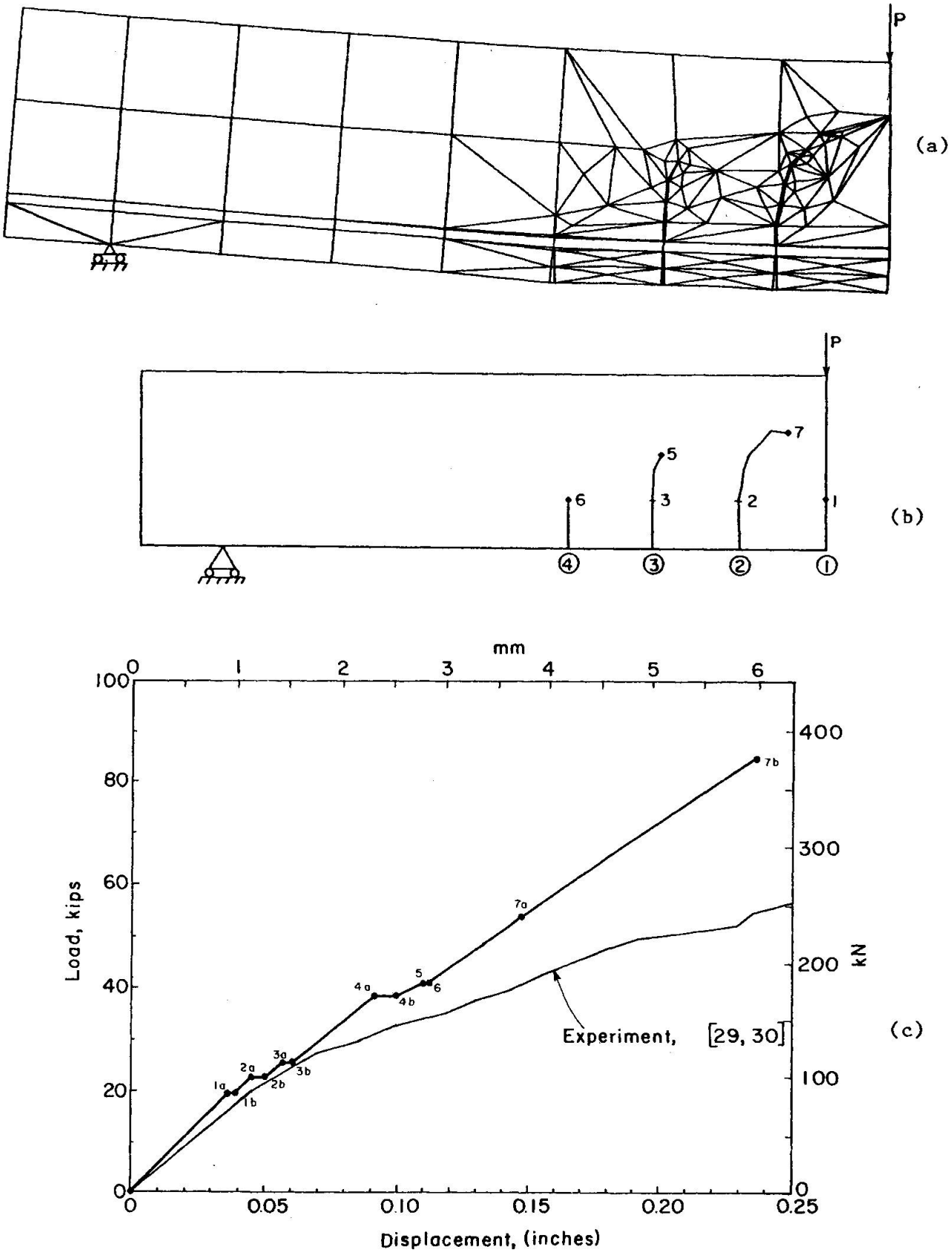

Fig. 10 Results of Analysis L-AI-1200. a) Final Mesh on Deflected Shape b) Final Crack Pattern c) Comparison of Calculated and Observed Load-Displacement Curves.

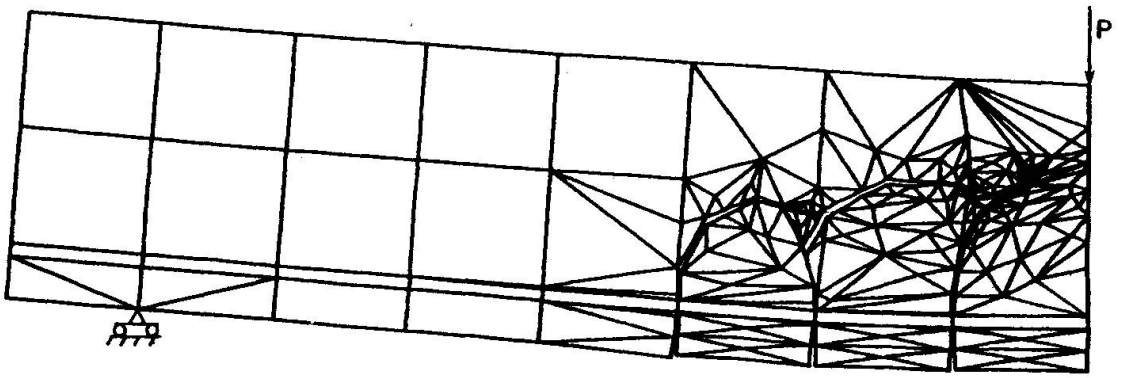

(a)

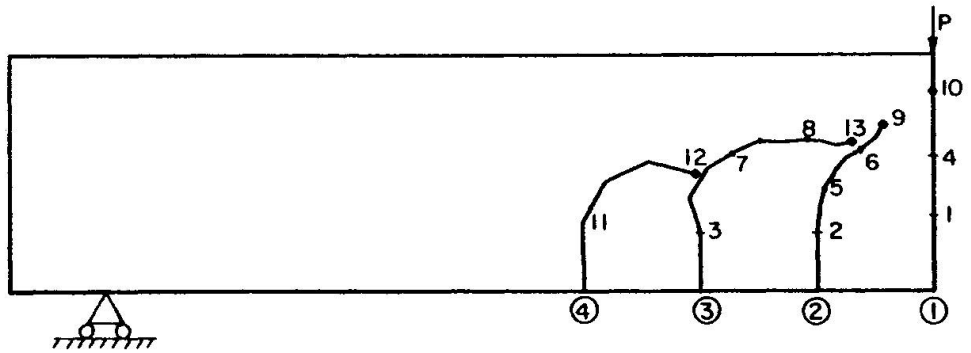

(b)

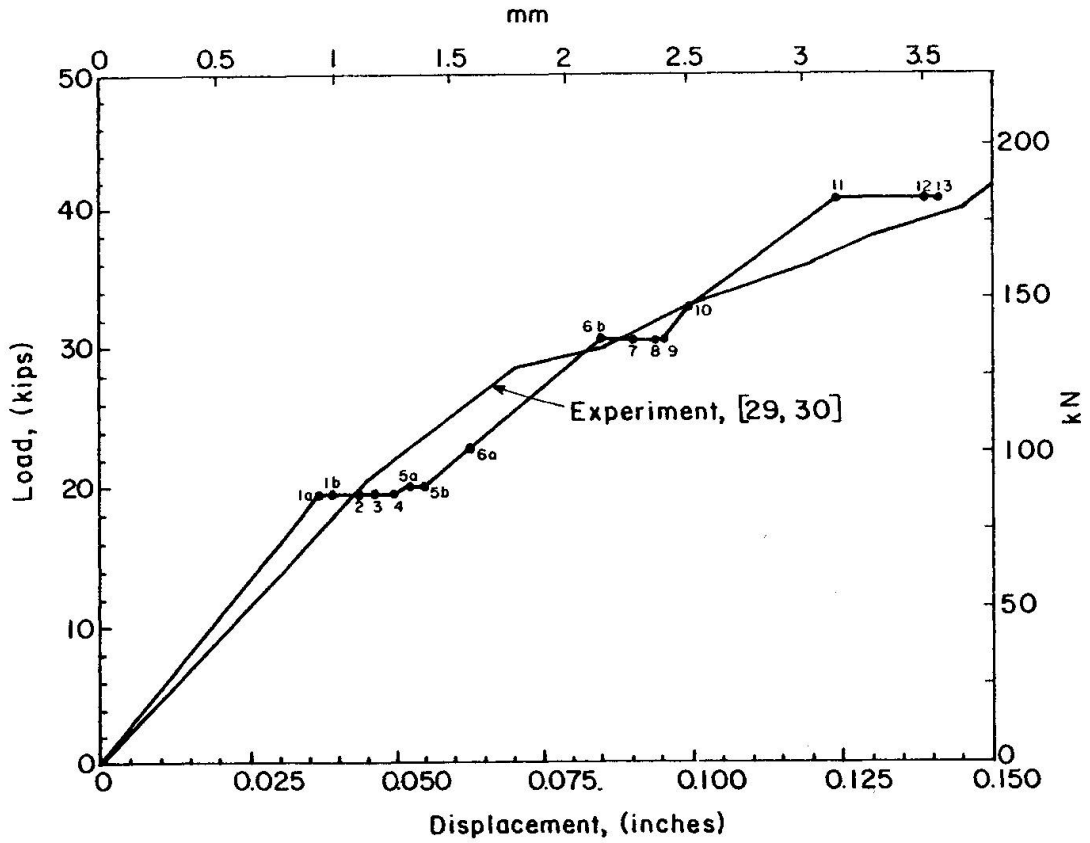

(c)

Fig. 11 Results of Analysis L-NAI-600. a) Final Mesh on Deflected Shape b) Final Crack Pattern c) Comparison of Calculated and Observed Load-Displacement Curves.

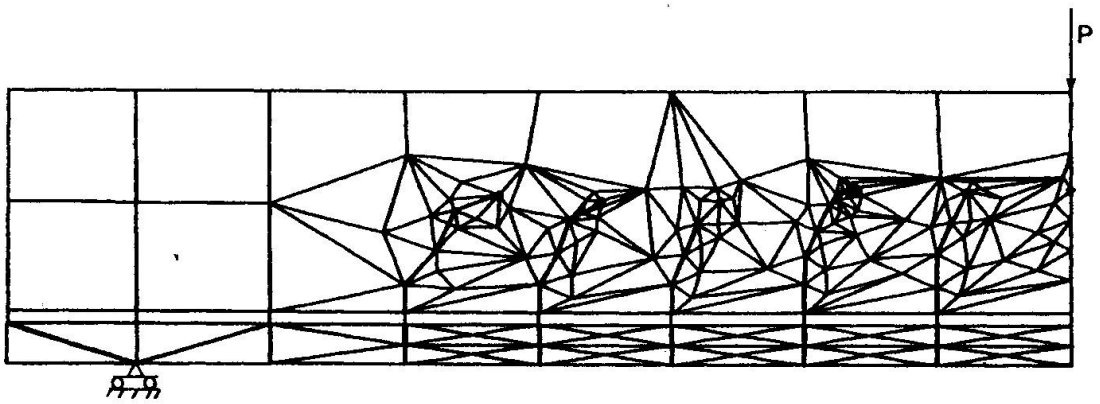

(a)

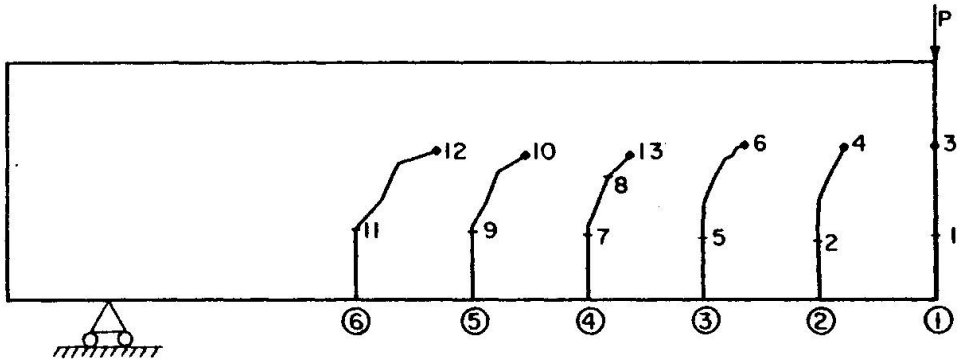

(b)

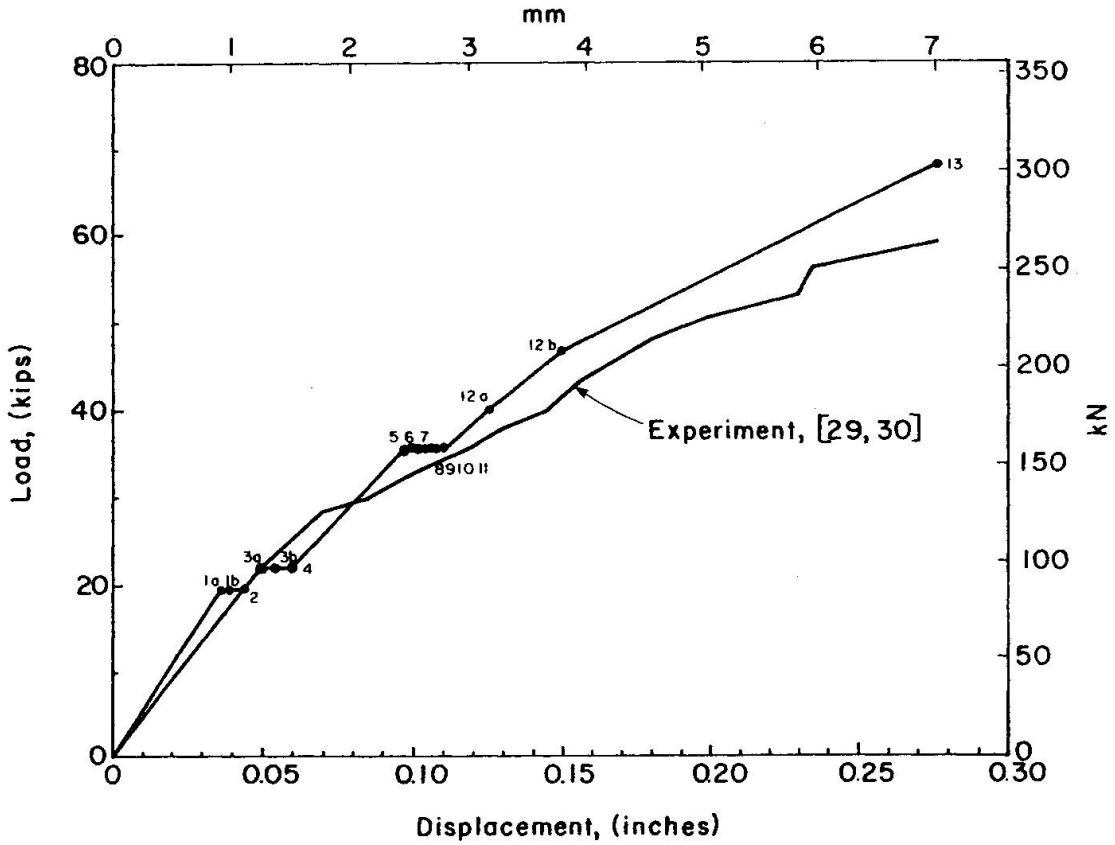

(c)

Fig. 12 Results of Analysis NL-AI-600. a) Final Mesh b) Final Crack Pattern c) Comparison of Calculated and Observed Load-Displacement Curves.

It appears that the absence of interface elements along a crack, modelling the aggregate interlock shear transfer, increases both K_I and K_{II} (as reflected by the large amount of cracking for a comparatively low load), and the ratio of K_{II}/K_I (as reflected by the large curvature of the cracks).

The softer response exhibited by this analysis is not surprising since no stiffness was present along the cracks to reduce the shear displacements.

Based on the final crack configuration, it seems reasonable to conclude that modelling of the shear transfer along cracks is an important factor. This conclusion agrees with Cedolin [31], who reached it based on a different criterion. He found substantial differences in the load displacement curves obtained through a parametric study of the shear modulus along a smeared crack.

4. The last, non-linear analysis, Fig. 12, is certainly the most accurate and satisfactory one. Good correlation between the experimental and numerical results is achieved all along the load path. The approach followed by the code to determine the load at the end of an increment makes it difficult to accurately predict the failure load (assumed to occur whenever a Gauss point will have its Young's modulus equal to zero) which can explain some of the small error in its predicted value. In fact, recalling that the code computes the load causing a crack to extend a certain predetermined length, one should select progressively smaller crack increments as the crack tips approach the compressive region. A selected length which may be too large will force the crack to enter the compressive region resulting in an unrealistically large load increase.

5. It is interesting to compare the relative contributions to the overall nonlinearity due to cracking (geometrical) and concrete softening (material), since no such comparison could be performed in a smeared crack approach.

To achieve such a comparison, for different load values, it has been assumed that the total displacement is a linear function of the 1) elastic response, 2) cracking and 3) concrete softening. The first contribution is obtained by extrapolating the initial stiffness of the uncracked beam in analysis L-AI-600. The second one is determined by subtracting the results of L-AI-600 from the first one,,and the last component by subtracting results of L-AI-600 from those of NL-AI-600. A normalized plot of the three contributions is shown in

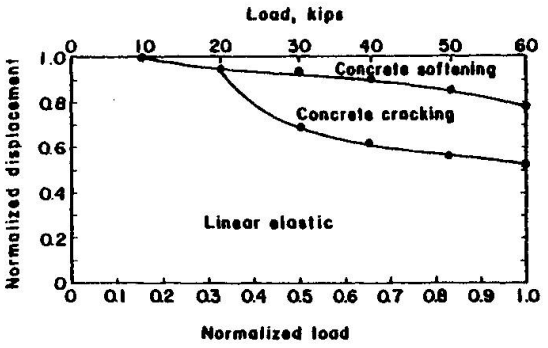

Fig. 13 Relative Contributions to Displacement Under the Load on Beam OA-1

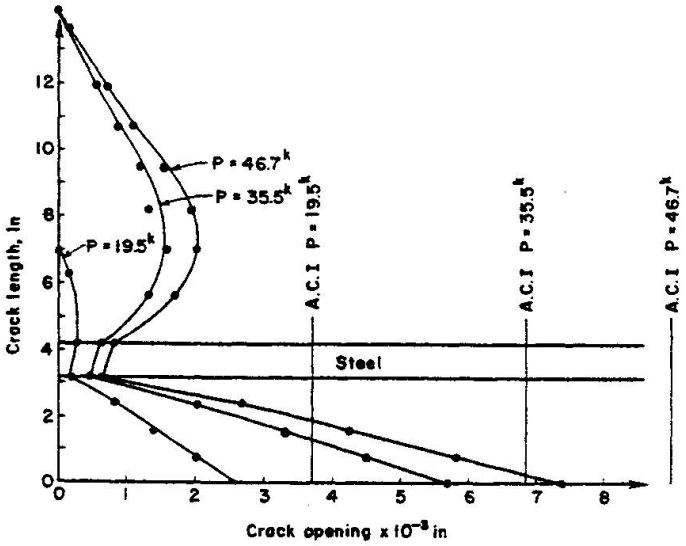

Fig. 14 Comparison Between Empirical and Calculated COD for Center Crack of Beam OA-1

Fig. 13. The most important observation indicated by this diagram is that once a crack has formed [at a load of about 20 kips (89 KN)], the cracking contribution throughout the whole range of loading is about 27 percent. It is not until about 70 percent of the failure load has been reached that concrete non-linearity starts to account for more than 10 percent, and at no time does the material non-linearity contribution exceed the geometrical one (22 percent as opposed to 26 percent at failure).

Of course no generalization could be made from this particular analysis, but the trend is a clear indication of the primary sources of non-linearity in a reinforced-concrete structure, and what their relative contributions are.

6. Another comparison which the smeared crack approach cannot perform is the measurement of the crack opening displacements. While those values were not reported in [29,30], a comparison with the ACI 318-77 Code [32] equation for crack opening is possible.

The center crack of NL-AI-600 has been selected, and its opening at three different load stages compared with the empirical ACI equation based on the experimental work of Gergely and Lutz, [33] Fig. 14.

The empirical equation overestimated the maximum crack opening at the lower fibers of the beam by 42, 19 and 21 percent under loads of 19.5, 35.5 and 46.7 kips (87, 158, and 208 KN), respectively. This percentage of error is certainly small in terms of engineering accuracy for an empirically derived formula for reinforced concrete.

Another interesting observation, which again could be done only through a discrete crack finite element analysis, is the shape of the crack opening. While the actual opening at the level of the steel bar is very much dependent upon the bond stiffness, it is nevertheless an order of magnitude smaller than the one occurring at the free surface.

7. Finally, it should be mentioned that the execution time of FEFAP is not prohibitively expensive as compared to the currently available codes using the smeared crack approach. Cedolin [31], reported a total CPU time of 1120 sec. on a UNIVAC 1108 for an analysis of the same beam problem, while the CPU time of the NL-AI-600 analysis was 460 sec. on an IBM 370/168 model 3 (estimated to be six times faster than the UNIVAC 1108).

6. DISCUSSION

Certain characteristics of FEFAP, positive and negative, merit discussion. On the positive side, it needs to be emphasized that the initial data set for the above example problem consisted of 30 card images, and that was all the data ever generated and entered into the computer by the analyst. All remeshing and renumbering was done automatically, quickly, cheaply, and without the possibility of human error.

Secondly, the interactive nature of FEFAP puts the analyst back into the analysis. With each increment of loading, the analyst is informed graphically of resultant changes in material properties and mesh topology, and immediately sees their effect on the load-displacement response of the structure. Moreover, since the program can be restarted from a previous crack increment at any time, parametric studies which highlight the effect of change in a particular variable on structural response can be easily performed.

Finally, it is clear that progressive cracking and material nonlinearity make a reinforced concrete structure increasingly difficult to analyze; the structure

is much more complex, topologically and constitutively, near failure than when unloaded. Yet, in the standard smeared crack approach to analysis, the initial mesh is the final mesh. This forces the analyst either to compromise accuracy at later stages of loading for cost-effectiveness at the initial stages when a complex mesh is unnecessary, or to carry a very fine mesh all the way through the analysis thereby incurring an initial inefficiency. The present approach is a natural one from the point of view of accuracy, as well as rigor. As the topology becomes more complex more elements are added as needed, yet no sacrifice in the rational fracture mechanics approach to crack propagation is made.

There are, however, some significant drawbacks in the operation of the current version of FEFAP. These fall into two general categories, topology and material modelling. Figs. 9 through 12 show that cracks currently can nucleate only from corner nodes of elements. This is an artificial and inaccurate constraint on crack modelling. These figures also show that a burden of many unnecessary elements behind the crack tip area is carried through the analysis. As mentioned above, the number of elements should increase with cracking, but not to the unnecessary degree presently seen.

As mentioned in Section 5.2.2, the current algorithm for modelling of material non-linearity is basically purely incremental, with no iteration capability to reduce unbalanced nodal loads. The inaccuracy introduced by this shortcoming is especially evident in the last load increment of analysis NL-AI-600, Fig. 12.

These and other minor drawbacks in the current version of FEFAP are the subject of ongoing improvement of the code. Example problems evincing their solution will be detailed during the oral presentation of this paper.

Finally, the authors would like to offer some philosophical comments concerning objectivity and the need for a rigorous, fracture mechanics approach to cracking. There are clearly, many classes of problems in reinforced concrete in which a tensile-strength-controlled, smeared crack approach to analysis is sufficiently accurate. It is also likely that there are some in which it is not. There can be no doubt that problems involving crack propagation in plain concrete structures, such as dams [34], must be approached with the objective tool of fracture mechanics. The key element in this issue is the crack arresting character of the reinforcement; in a given structure, if the layout and strength of the reinforcement, and the capacity of bond to transmit stress to it, are sufficient to arrest cracks and maintain their local stability throughout the course of loading, then it is likely that the currently popular approach is sufficiently accurate. If not, then the proposed approach is necessary.

In light of these final comments, the authors suggest that an international "Blind Round-Robin" testing analysis program be formed. A series of well controlled and documented laboratory or field tsts on various types of structures would be performed in Europe and the United States. Concurrently, various research groups will analyze the same structures using the approach of their choice. An international symposium would then bring together experimentalists, analysts, and their results for comparison and discussion.

This initiative would give new impetus to a field with rapidly expanding applications, but in which significant new development has not occurred for nearly a decade.

7. CONCLUSIONS

A completely new and comprehensive solution methodology to the problem of modelling discrete crack propagation in reinforced concrete was presented. An interactive computer code, FEFAP, was developed which uses linear elastic

fracture mechanics principles to govern mixed-mode crack propagation. A new mesh is generated and renumbered automatically, quickly, and cheaply, after each topology change. The following conclusions concerning FEFAP and its bases are drawn:

1. The example reinforced concrete problem analyzed shows that:

   i) Concrete fracture toughness value does not play a dominant role in the load displacement response.

   ii) Aggregate interlock must be modelled.

   iii) Most of the overall structural non-linearity stems from concrete cracking, and only toward failure does concrete softening play a substantial role.

   iv) FEFAP costs about the same to run on a given problem as codes using a smeared crack approach.

2. The most important advantages that the discrete-crack, fracture mechanics model has over the smeared crack model are:

   i) Rational and rigorous criteria for stability, direction, and length of a crack increment.

   ii) Accurate determination of crack tip location.

   iii) Evaluation of crack opening displacements.

   iv) Breakdown of nonlinearity into its two components, cracking and softening.

   v) Control of the strain energy gradient within each element throughout the analysis due to the local remeshing along the crack and around its tip.

   vi) Capability of using rational models for aggregate interlock along the cracks.

3. Interactive mode of analysis through a storage tube display device (medium level computer graphics) is found to be a very efficient mode of operation. Information which would otherwise require pages of output and hours of study of printed forms is displayed continuously and quickly. Furthermore, the analyst can inject his engineering judgment into the analysis within a "friendly" working environment.

It is hoped that the initial success of the fracture-mechanics, discrete crack approach will stimulate more research and applications not only in reinforced concrete but in other structural materials as well.

8. ACKNOWLEDGMENTS

The authors would like to thank Professors Peter Gergely and Richard White for their assistance and encouragement in this research. The financial support of the National Science Foundation under Grant PFR7900711 to Cornell University is gratefully acknowledged. The first author also extends thanks to the Interactive Computer Graphics Laboratory of Princeton University for their technical support in some parts of the program development.

9. REFERENCES

1. Bazant, Z.P., "Advances in Deformation and Failure Models of Concrete," Introductory Report, IABSE Colloquium on Advanced Mechanics of Reinforced Concrete, Delft, 1981, pp. 9-37.

2. Argyris, J.H., Faust, G., and Willam, K.J., "Finite Element Modelling of Reinforced Concrete Structures," Introductory Report IABSE Colloquium on Advanced Mechanics of Reinforced Concrete, Delft, 1981, pp. 85-106.

3. Bazant, Z.P., Cedolin, L., "Blunt Crack Band Propagation in Finite Element Analysis," J. of the Engineering Mechanics Div., Proc. ASCE, Vol. 105, No. EM2, April 1979, pp. 297-315.

4. Argyris, J.H., Faust, G., and Willam, K.J., "Finite Element Analysis of Concrete Cracking," ISD-Report No. 254, Stuttgart, 1979.

5. Saouma, V., Ingraffea, A.R., Catalano, D., "Fracture Toughness of Concrete - K_{Ic} Revisited," Dept. of Structural Engineering Report 80-9, Cornell University, 1980.

6. Ingraffea, A.R., and Schmidt, R.A., "Experimental Verification of a Fracture Mechanics Model for Tensile Strength of Indiana Limestone," Proc. 19th U.S. Symposium on Rock Mechanaics, Stateline, Nevada, 1978, pp. 247-253.

7. Schmidt, R.A., and Lutz, T.J., "K_{Ic} and J_{Ic} of Westerly Granite--Effect of Thickness and In-Plane Dimensions," ASTM STP678, 1979, pp. 166-182.

8. Catalano, D., "A Linear Elastic Fracture Mechanics Approach to Toughness of Concrete," M.S. Thesis, Dept. of Structual Engineering, Cornell University, 1981.

9. Schmidt, R.A., "A Microcrack Model and Its Significance to Hydraulic Fracturing and Fracture Toughness Testing," Proc. 21st U.S. Symposium on Rock Mechanics, Rolla, Missouri, 1980.

10. Erdogan, F., and Sih, G.C., "On the Crack Extension in Plates Under Plane Loading and Transverse Shear," ASME J. Basic Engineering, V. 85, 1963, pp. 519-527.

11. Hussain, M.A., Pu, S.L., and Underwood, J.H., "Strain Energy Release Rate for a Crack Under Combined Mode I and Mode II," Fracture Analysis, ASTM, STP560, 1974, pp. 2-28.

12. Sih, G.C., "Strain-Energy-Density Factor Applied to Mixed-Mode Crack Problems," Int. J. of Fracture Mechanics, V. 10, No. 3, 1974, pp. 305-321.

13. Barsoum, R.S., "On the Use of Isoparametric Finite Elements in Linear Fracture Mechanics," Int. J. of Numerical Methods in Engineering, V. 10, No. 1, 1976, pp. 25-37.

14. Henshall, R.D., and Shaw, K.G., "Crack Tip Elements are Unnecessary," Int. J. of Numerical Methods in Engineering, V. 9, 1975, pp. 495-509.

15. Ingraffea, A.R., Heuze, F.E., "Finite Element Models for Rock Fracture Mechanics," Int. J. for Numerical and Analytical Methods in Geomechanics, V. 4, 1980, pp. 25-43.

16. Shih, C.F., de Lorenzi, H.G., and German, M.D., "Crack Extension Modeling with Singular Quadratic Isoparametric Elements," Int. J. of Fracture, V. 12, 1976, pp. 647-651.

17. Lynn, P.P., and Ingraffea, A.R., "Transition Element to be Used With Quarter-Point Crack Tip Elements," Int. J. of Numerical Methods in Engineering, Vol. 12, No. 6, 1978, pp. 235-248.

18. Ingraffea, A.R., and Manu, C., "Stress-Intensity Factor Computation in Three Dimensions With Quarter-Point Elements," Int. J. for Numerical Methods in Engineering, Vol. 15, No. 10, 1980, pp. 1427-1445.

19. Goodman, R.E., Taylor, R.L., and Brekke, T.L., "A Model for the Mechanics of Jointed Rock," J. of the Soil Mechanics Div., ASCE, SM3, 1968, pp. 637-659.

20. Ngo, D., "A Network-Topological Approach for the Finite Element Analysis of Progressive Crack Growth in Concrete Members," Ph.D. Dissertation, Div. of Structural Engineering and Structural Mechanics, University of California, Berkeley, UC-SESM 75-6, 1975.

21. Ottosen, N.S., "A Failure Criterion for Concrete," J. of the Engineering Mechanics Div., ASCE, Vol. 103, No. EM4, 1977, pp. 527-535.

22. Ottosen, N.S., "Constitutive Model for Short-Time Loading of Concrete," J. of the Engineering Mechanics Div., ASCE, Vol. 105, No. EM1, 1979, pp. 127-141.

23. Nilson, A.H., "Bond Stress-Slip Relations in Reinforced Concrete," Report No. 345, Dept. of Structural Engineering, Cornell University, 1971.

24. Fenwick, R.C., and Paulay, T., "Mechanics of Shear Resistance of Concrete Beams," J. of the Structural Div., ASCE, V. 94, No. ST10, 1968, pp. 2325-2350.

25. Everstine, G., "A Comparison of Three Resequencing Algorithms for the Reduction of Matrix Profile and Wavefront," Int. J. of Numerical Methods in Engineering, V. 14, 1979, pp. 837-853.

26. Gibbs, N.E., Poole, W.J., and Stockmeyer, P.K., "An Algorithm for Reducing the Bandwidth and Profile of a Sparse Matrix," SIAM J. of Numerical Analysis, V. 13, 1976, pp. 236-250.

27. Chang, S.C., "An Integrated Finite Element Nonlinear Shell Analyusis System with Interactive Computer Graphics," Ph.D. Dissertation, School of Civil and Environmental Engineering, Cornell University, 1981.

28. Saouma, V.E., "Finite Element Analysis of Reinforced Concrete: A Fracture Mechanics Approach," Ph.D. Disseration, School of Civil and Environmental Engineering, Cornell University, 1981.

29. Bresler, B., and Scordelis, A.C., "Shear Strength of Reiforced Concrete Beams," Structures and Materials Research Department of Civil Engineering, Series 100, Issue 13 (SESM 61-13), Institute of Engineering Research, University of California, Berkeley, 1961.

30. Bresler, B., and Scordelis, A.C., "Shear Strength of Reinforced Concrete Beams," J. of the American Concrete Institute, V. 60, No. 1, 1963, pp. 51-74.

31. Cedolin, L., and Dei Poli, S., "Finite Element Studies of Shear Critical R/C Beams," J. of the Engineering Mechanics, Div., ASCE, Vol. 103, No. EM3, 1977, pp. 395-410.

32. ----, "Building Code Requirements for Reinforced Concrete (ACI 318-77)", American Concrete Institute, Detroit, 1977.

33. Gergely, P., and Lutz, L., "Maximum Crack Width in Reinforced Concrete Flexural Members," Causes, Mechanisms and Control of Cracking in Concrete, ACI Publ. SP-20, 1968, pp. 1-17.

34. Chappell, J., "A Fracture Mechanics Investigation of the Cracking of Fontana Dam," Report No. 81-7, Dept. of Structural Engineering, Cornell University, 1981.